© 2020. Published by The Company of Biologists Ltd | Journal of Experimental Biology (2020) 223, jeb220277. doi:10.1242/jeb.220277

RESEARCH ARTICLE

Mechanical fatigue fractures bivalve shells

R. L. Crane* and M. W. Denny

ABSTRACT

Mollusk shells protect against diverse environmental and predatory physical threats, from one-time impacts to chronic, low-magnitude stresses. The effectiveness of shells as armor is often quantified with a test of shell strength: increasing force is applied until catastrophic fracture. This test does not capture the potential role of fatigue, a process by which chronic or repeated, low-magnitude forces weaken and break a structure. We quantified the strength and fatigue resistance of California mussel (*Mytilus californianus*) shells. Shells were fatigue tested until catastrophic failure by either loading a valve repeatedly to a set force (cyclic) or loading a valve under constant force (static). Valves fatigued under both cyclic and static loading, i.e. subcritical forces broke valves when applied repeatedly or for long durations. Stronger and more fatigue-resistant valves tended to be more massive, relatively wider and the right-hand valve. Furthermore, after accounting for the valves' predicted strength, fatigue resistance curves for cyclic and static loading did not differ, suggesting that fatigue fracture of mussels is more dependent on force duration than number of cycles. Contextualizing fatigue resistance with the forces mussels typically experience clarifies the range of threats for which fatigue becomes relevant. Some predators could rely on fatigue, and episodic events like large wave impacts or failed predation attempts could weaken shells across long time scales. Quantifying shell fatigue resistance when considering the ecology of shelled organisms or the evolution of shell form offers a perspective that accounts for the accumulating damage of a lifetime of threats, large and small.

KEY WORDS: *Mytilus californianus*, Cyclic loading, Functional morphology, Mollusk, Mussel, Strength

INTRODUCTION

The rigid, external shells of many mollusks provide protection against a lifetime of diverse threats. Defending mollusks from predators attempting to drill, crush, peel or pry them open, and from environmental insults, such as wave-hurled projectiles (Shanks and Wright, 1986), shells are an impressive armor. With their diverse forms and extensive fossil record, they can provide unique evolutionary insight, and their fracture-resistant forms and microstructures inspire contemporary biomimetic ceramics (Pro and Barthelat, 2019). Most research that quantifies shell mechanics focuses on whether high-magnitude forces are sufficient to immediately break a shell (e.g. Blundon and Vermeij, 1983; Fisher, 2010; Preston et al., 1996; Vermeij and Currey, 1980), paying less attention to encounters that have no apparent consequences. In this study, we explored a broader range of threats, from single potentially lethal forces to the chronic low-magnitude stresses of daily existence that might cause accumulating, unseen damage.

In order to quantify the effectiveness of shells as armor, researchers often rely on a test in which a shell is compressed under an increasing force until it fractures (method described in Vermeij and Currey, 1980). The force at failure defines the strength, or one-time breaking force. (In an engineering sense, strength, as classically defined, is the stress at failure, or the force per cross-sectional area in the structure at breakage. However, we adhere to a less formal definition of strength as force, a definition often found in discussions of biological structures.) Strength tests provide a tool to compare different mollusk populations (e.g. Blundon and Vermeij, 1983; Bourdeau, 2010; Fisher, 2010; Gaylord et al., 2011; Vermeij and Currey, 1980) and to quantify the threat from specific predators (e.g. Buschbaum et al., 2007; Kolmann et al., 2015; Preston et al., 1996).

Strength tests offer insight into the high-magnitude forces that immediately break shells, but they do not address the significance of lower magnitude forces that mollusks encounter on a daily basis. Low-magnitude forces, if applied repeatedly (cyclically), can weaken and ultimately break a structure through the process of fatigue (reviewed in a biological context in Mach et al., 2007). Fatigue occurs as damage accumulates: microscopic flaws ('cracks') in a structure extend at subcritical forces (process described in Gosline, 2018). More specifically, any crack will cause a local concentration of stress at the crack tip that exceeds the stress imposed on the structure as a whole. This local stress can cause the crack to propagate slightly. As the crack extends incrementally, the local stress at its tip is amplified, further weakening the structure. Thus, as microfractures extend and accumulate, the structure fatigues, until cracks propagate catastrophically, at which point a force well below the one-time breaking force is sufficient to break the shell. Fatigue causes failure in a variety of biological structures, including bone (Caler and Carter, 1989; Currey, 1998; Zioupos et al., 2001), algae (Denny et al., 2013; Mach, 2009; Mach et al., 2011) and tendon (Wang et al., 1995).

Mollusk shells have also been shown to fatigue (Boulding and LaBarbera, 1986; Currey and Brear, 1984; LaBarbera and Merz, 1992). However, these studies have focused primarily on relatively high forces (≥65% of the one-time breaking force) and relatively low cycle numbers (mostly <1000), as they have considered fatigue in the context of predation. A few studies have also examined how repeated impacts damage mollusk shells (Crane et al., 2018; Taylor, 2016), but again, these have focused on a few, high-force impacts (<120 impacts). None of this research has developed a broader framework to examine how a wide range of potentially fatiguing forces affects animal survival.

Considering a broader range of threats also raises the question of what role the duration of force application plays in the course of fatigue. Mollusks confront forces that range in duration from transient impacts, as from wave-hurled debris, to chronic loads, such as those imposed by jostling neighbors in a tightly packed mussel bed. Classically, fatigue encompasses damage specifically due to

Hopkins Marine Station of Stanford University, Pacific Grove, CA 93950, USA.

*Author for correspondence (rlcrane@stanford.edu)

R.L.C., 0000-0002-2438-4091; M.W.D., 0000-0003-0277-9022

Received 13 December 2019; Accepted 9 April 2020

Journal of Experimental Biology (2020) 223, jeb220277. doi:10.1242/jeb.220277

repeated loading, and the time course of fatigue depends on the number of cycles independent of the duration of each cycle (reviewed in Suresh, 1998). In accord with this definition, fatigue in some biological structures has been shown to be primarily cycle dependent (Caler and Carter, 1989; Mach, 2009; Moore et al., 2004). However, other biological structures, when loaded cyclically, experience time-dependent fatigue, breaking after a certain duration of loading regardless of the number of cycles (Caler and Carter, 1989; Carter and Caler, 1983; Zioupos et al., 2001), and fatigue in yet other structures depends on both cycle number and duration (Wang and Ker, 1995; Wang et al., 1995). In mollusk shells, the relative importance of cycle number and duration in determining fatigue has not, to our knowledge, been explicitly studied.

Shells of the California mussel, *Mytilus californianus*, are an ideal system to study the importance of fatigue. Mussels are abundant and have a relatively simple, and therefore tractable, morphology: a shell composed of two domed valves joined by a hinge on the dorsal side (Fig. 1A). Like other bivalves, their shell comprises crystals of calcium carbonate in an organic matrix, organized in layers with distinct microstructure. Furthermore, the California mussel and other *Mytilus* species are well studied, being of both economic significance for aquaculture and ecological significance as a key player in the intertidal zone of rocky shores. Mussels create tightly packed beds that provide substrate and protection for a multitude of organisms (Suchanek, 1979), while competing with other macrofauna for limited primary substrate (Dayton, 1971; Paine, 1966).

In this study, we asked whether shells of the California mussel fatigue, and across what forces and time scales. Fatigue has been demonstrated in mollusk shells at high forces, but the fatigue response at lower forces across longer time scales is undescribed. We addressed this question with strength tests of mussel valves as well as fatigue tests across a broad range of forces, under both cyclic loading, in which a set load was repeatedly applied and removed until fracture, and static loading, in which a set load was applied and maintained until fracture. From our mechanical results, we asked three more specific questions. First, does fatigue occur on ecologically relevant time scales? By comparing mechanical results with the forces mussels encounter in the wild, we can identify contexts likely to contribute to fracture. Second, what morphological features are associated with strength and fatigue resistance? By affecting stress distributions, certain shell forms may confer more fracture resistance. Finally, how do different loading regimes contribute to fatigue? Classically, cycle number is thought to determine the time course of fatigue more than loading duration.

MATERIALS AND METHODS

Animal collection and maintenance

Mussels (*Mytilus californianus* Conrad 1837) were collected at Hopkins Marine Station, Pacific Grove, CA, USA (Scientific Collecting Permit nos SC-13854 and S-190720016-19072-001) from a single site [0.32–0.75 m above mean lower low water (MLLW), 36.62193°N, 121.90521°W], and housed in a flow-through seawater system. It is impossible to know the accumulated forces encountered by each mussel before testing, but we limited variation by collecting all mussels from a single bed and including only mussels with minimal damage, defined as the majority of the periostracum intact, no external damage for which nacre was visible and no more than approximately 3 mm^2 of the internal surface area showing repair or patching.

Mechanical testing

Shell preparation and measurements

Mussels were killed, measured and prepared for subsequent testing. A scalpel was used to sever the posterior adductor muscle, and the valves were carefully separated. Tissue was gently pushed out of each shell with a blunt probe. Valve length, width, height and thickness at the hinge were measured (digital calipers with 0.01 mm resolution; see Fig. 1A for definitions), and each valve was patted dry and weighed (0.001 g resolution, AW120, Shimadzu Corp., Kyoto, Japan). To prepare for mechanical testing, the aperture was minimally sanded (320–400 grit) by hand to lie flat against the testing plate. This procedure removed only the small bumps and ridges that often occur along mussel apertures. Shells were stored in saltwater between all steps and after preparation until testing, and they were always tested within 24 h of mussels being killed and within 14 days of being collected. There were no differences in the preparation or storage of left and right valves.

Experimental design

We took advantage of mussels' two-valved morphology to design three paired experiments. (1) We measured the strength of both valves (N=64 pairs of valves, i.e. both valves from 64 mussels; length: mean±s.d. 29.4±4.0 mm, range 21.3–37.6 mm). (2) We measured the strength of one valve and the cyclic fatigue resistance

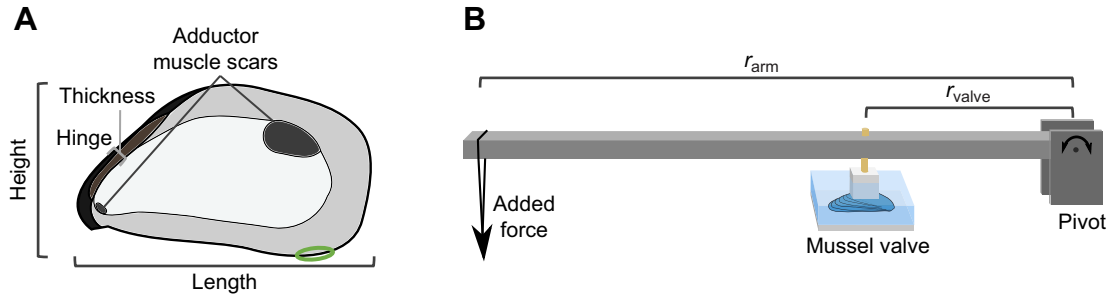

Fig. 1. Mussel morphology and experimental set-up. (A) Internal structures of a right valve of a California mussel. Length, height and hinge thickness were measured as the maximum extent along the defined axes. Width was measured as the widest extent perpendicular to height and length. The green oval indicates the approximate location of the hook used when measuring maximum closing force. The valve is oriented with anterior to the left and dorsal above. (B) During static fatigue testing, a force was applied to a mussel valve in a saltwater bath by adding a force at the end of a lever arm. The force applied to the shell was calculated according to Eqn 1, with r_{valve} and r_{arm} defined as the length of the radius arm from the pivot to the valve and to the applied force, respectively. This apparatus was adapted to test the constant opening force generated by the mussel hinge. Not to scale; the lever arm was proportionally longer and the mussel smaller than portrayed here.

of the other (N=103 pairs of valves; length: mean±s.d. 31.6±3.0 mm, range 25.1–39.2 mm). (3) We measured the strength of one valve and the static fatigue resistance of the other (N=71 pairs of valves; length: mean±s.d. 31.3±3.4 mm, range 22.5–41.0 mm). For testing details, see below. Although the term 'fatigue' often refers only to cyclic loading (reviewed in Suresh, 1998), we here expand the term, using 'static fatigue' to delineate fracture under constant loads, as in Gosline (2018).

Experimental treatments for the left versus right valve were assigned haphazardly. For fatigue experiments, the maximum fatiguing force was also determined haphazardly (cyclic fatigue force range 75–591 N; static fatigue force range 74–212 N). During all testing, valves were fully submerged in saltwater (19±4°C).

Strength testing

Strength was measured by compressing valves with an increasing force between two flat plastic plates (Delrin® acetal resin on top and PVC underneath) until catastrophic failure. The increasing force was applied from above with a hydraulic ram (PLA Series, Parker Electrohydraulics, Elyria, OH, USA) controlled by a 0–10 V signal from a 16-bit analog/digital board (USB-6211, National Instruments, Austin, TX, USA).

The applied force was measured with a force plate. The valve rested on the top plate of the force sensor. As the valve was compressed, the top plate would move downward, compressing a 5.08 cm long die spring (chrome-silicon steel with ground and closed ends, rate 88.58 kg cm^{-1}) and moving the center core of a linear variable differential transformer (HR 100, Schaevitz Sensors, Hampton, VA, USA), the voltage output of which ran through the analog/digital board to the computer. The force plate was calibrated with items of known weight.

A series of scripts in MATLAB (version R2017b, MathWorks, Natick, MA, USA) drove the hydraulic arm and synchronized data collection from the force sensor. The ram moved at a constant linear velocity of 15.2 mm s^{-1} to a maximum displacement that would correspond to a load of 656 N, if the valve did not break. The range of shell sizes was determined such that all valves broke under this loading regime. From the loading curve, the one-time breaking force was identified as the force at catastrophic failure.

During strength testing, five valves broke at forces below 68 N, three standard deviations below the average strength. We interpreted these uncharacteristic weaknesses as indicating pre-existing damage, and we therefore excluded these valves and their paired counterparts (N=1 from paired strength experiments, N=1 from cyclic fatigue experiments, N=3 from static fatigue experiments).

Cyclic fatigue testing

During cyclic fatigue testing, valves were loaded repeatedly until catastrophic failure to a pre-determined force using the same experimental setup described in 'Strength testing', above. Specifically, valves were compressed by the hydraulic ram, moving to a pre-determined position corresponding to the target force at a constant linear velocity of 15.2 mm s^{-1}. Valves were then immediately unloaded at the same velocity. In this way, the total time of each loading and unloading cycle ranged between 0.25 and 1.03 s depending on the maximum force (range 75–591 N). The duration of each loading/unloading cycle for a given valve was consistent.

In order to reach a consistent maximum force across many cycles, the MATLAB program driving the hydraulic ram could identify and adjust to any accumulated deformation in the valve or testing apparatus. Thus, the applied force for an experiment is defined as the median of the maximum force for each cycle, excluding the cycle during which the valve broke. Because it was important to load to the same force on each cycle, valves were excluded if the range of cycle maxima exceeded 50 N (N=5 valves). This limited the variation of cycle maxima in each experiment [s.d. of maxima relative to median maximum force across all cycles for that valve: median (IQR): 1.3% (0.8%, 1.8%), range: 0.3–8.2%].

A brief lag was necessary between each loading/unloading cycle for MATLAB to determine whether the valve had broken (time lag: median 0.24 s, range 0.19–0.47 s). The valve was not loaded during this lag. Additionally, if MATLAB needed to adjust the ram position, which occurred in 0.3% of cycles, a longer delay was necessary (time lag: median 7.9 s, range 5.4–16.9 s).

Because of time constraints, four experiments had to be stopped prematurely, before the valve had broken. These valves are indicated in figures but are not included in analyses, as the true number of cycles until failure is unknowable.

Static fatigue testing

To test the role of duration in fatigue, valves were compressed under a constant load until catastrophic failure. The load was applied by hanging known weights from the end of a lever arm (2.54 cm square aluminium tubing, 0.3175 cm thick, 92 cm long) under which the valve was compressed between two plastic plates (Delrin® acetal resin; Fig. 1B). An Arduino microcontroller and switch recorded the time elapsed between when the compressive force was initially applied and when each valve broke (Arduino Uno, Somerville, MA, USA). Valves that broke immediately after the weight was applied were excluded. Experiments were conducted in baths initially filled from a flow-through seawater system. Water level was maintained with the addition of tap water, thereby maintaining salinity.

We calculated the force applied to the valve during static loading (F_{valve}) by balancing the torques (force×radius) acting on the stationary lever:

$$F_{valve} r_{valve} = (F_{added} + F_{arm}) r_{arm}, \quad (1)$$

where r_{valve} and r_{arm} are the length of the radius arm from the pivot to the valve and to the applied force, respectively (Fig. 1B). F_{added} is the force from the added weight and F_{arm} is the force imposed by the lever arm, which was measured directly as the force required to hold the lever arm horizontal at r_{arm}.

Self-imposed forces

To place the results of the strength and fatigue tests in an ecological context, we measured the self-imposed forces of a mussel clamping shut. We bounded this range by measuring the typical force that mussels are constantly imposing on their shells and the maximum force mussels are capable of generating. Mussels were collected and maintained as described in 'Mechanical testing', above, and were tested within 36 h.

Minimum closing force

The mussel hinge acts as a torsional spring, constantly tending to open the shell, a force that can be counteracted by contraction of the adductor muscles (Fig. 1A). We quantified this constant, low-magnitude force by severing the posterior adductor muscle then measuring the force required to compress the shell until it closed (N=10 mussels; shell length: mean±s.d. 31.5±4.2 mm, range 27.9–42.4 mm).

Before the experiment, we used a Dremel rotary tool to create a small, round, superficial divot in the exterior, posterior, ventral

Journal of Experimental Biology (2020) 223, jeb220277. doi:10.1242/jeb.220277

quadrant of one valve (randomly determined) of each live mussel. Based on preliminary experiments, this location was chosen to eliminate slippage of the experimental device, and because the defined distance from the hinge, which we account for in torque calculations, resulted in both precise and speedy experiments. We then severed the posterior adductor muscle using a scalpel inserted ventrally between the valves, avoiding damage to the hinge. The shell was placed in a saltwater bath for at least 5 min to allow the hinge to fully open. Each shell was tested three times and was allowed to rest in a saltwater bath for at least 5 min between rounds.

During testing, shells were held in place with flexible molding clay and oriented with the aperture of the lower valve horizontal. The upper valve, with the superficial divot, was allowed to open. A slowly increasing force was then applied to the top valve at the location of the divot. The force was applied by dripping water at a controlled rate into a bucket hanging from the end of a lever arm (Fig. 1B). A wood screw pointing downward in the middle of the lever arm allowed us to apply the closing force to the divot. The rate at which the force increased varied across individual mussels depending on the location of the divot (and thus the length of the lever arm), but trials ran for approximately 20–160 s. The shell was visually monitored until it closed (i.e. there was no visible gap between the two valves), and the water-filled bucket was then immediately removed and weighed.

After the experiment, shells were measured as described in 'Shell preparation and measurements', above, and both the internal and external surfaces were photographed with the aperture parallel to the focal plane (2988×5312 pixel resolution). From the photographs, we measured the perpendicular distance from the rotational axis of the hinge to the divot and to the center of the posterior adductor muscle scar (Fig. 1A; ImageJ, version 1.51; Schneider et al., 2012), which was necessary to calculate the forces applied to the shell. First, from the final applied weight in each experiment, we calculated the force applied by the lever arm to the shell by taking the lever arm length into account as described in 'Static fatigue testing', above (Eqn 1). Then, to calculate the torque imposed by the hinge, we multiplied the force experimentally applied to the shell by the perpendicular distance from the hinge to the superficial divot. Finally, assuming the role the posterior adductor muscle played in closing the shell far outweighed the role of the much smaller anterior adductor muscle, we calculated the force required for the posterior adductor muscle to counteract the torque from the hinge using the radius arm length from the hinge to the posterior adductor muscle.

Maximum closing force

We measured the maximum closing force as the maximum force required to open a live, closed mussel (N=13 mussels; shell length: mean±s.d. 31.8±3.6 mm, range 24.3–40.7 mm; methods modified from Campbell, 1987).

At least 24 h before testing, each mussel was glued to a strip of plastic using Z-Spar epoxy. The shell was oriented with the lower aperture parallel to the plastic, and we randomly determined which valve was oriented downward. Animals were returned to tanks until testing.

During the experiment, a small metal hook was inserted under the posterior ventral side of the lip (Fig. 1A). The force was then monitored using a tension scale as an experimenter pulled slowly upward on the hook until the mussel just began to gape (by ∼1 mm). The force was then released, and the maximum force was recorded. Each animal was tested at least three times, resting for 30 s between rounds. Experiments were conducted in a saltwater bath at the same temperature as the flow-through tanks in which the animals were stored.

After testing, mussels were killed, measured and photographed as described above (see 'Mechanical testing'). From the photographs, we measured the perpendicular distance from the rotational axis of the hinge to the location where the hook was inserted (r_{hook}) and to the center of the posterior adductor muscle scar (r_{muscle}). We also measured the surface area of the muscle scar. From these measurements, and the measured force required to pry open the shell (F_{hook}), we calculated the maximum force the posterior adductor muscle was able to generate. We assumed the force applied by the posterior adductor muscle (F_{muscle}) far exceeded the force from any other musculature inside the shell, and we calculated the maximum force applied by the muscle as:

$$F_{muscle} = \frac{(F_{hook} r_{hook}) + \tau_{hinge}}{r_{muscle}}, \quad (2)$$

where τ_{hinge} is the torque applied by the hinge. We predicted the torque imposed by the hinge using a statistical model of hinge torque as a function of shell length described below (see 'Statistical analyses') and reported in Results.

Statistical analyses

Morphological scaling

Before conducting analyses of valve strength, we assessed the scaling of the linear morphological variables (length, height, width and thickness at the hinge). We tested whether the scaling exponent (b) from the allometric scaling equation:

$$y = ax^b \quad (3)$$

differed from the null hypothesis of b=1, as expected for isometric scaling of linear variables. Using log-transformed variables, we fitted reduced major axis regressions individually for valve height, width and thickness, each as a function of valve length (models fitted in R, lmodel2, version 1.7-3; https://CRAN.R-project.org/package=lmodel2), and we generated 95% confidence intervals for the slope (b) and determined whether b=1 was contained within those intervals. We fitted these models for valves that had been strength tested. For shells for which both valves were strength tested, we used measurements from the first valve to be tested to avoid complications from having multiple measures of some but not all mussels.

Strength testing

We assessed what morphological features were associated with valve strength. First, we conducted unpaired analyses of every valve whose strength was tested. For shells for which both valves were strength tested, we used the same subset of valves as for the morphological scaling analyses described above. We fitted a multiple regression of valve strength as a function of a variety of morphological variables: mass, domedness (width/length), relative thickness (thickness/length) and a categorical variable indicating right or left valve. We began with a full model including all variables, then excluded non-significant variables. Additionally, with the unpaired data, we compared morphological features of the right and left valves; we conducted Welch's two sample t-tests comparing the mass of the right and left valves and comparing the domedness of the right and left valves.

We also used paired data for which both valves had been strength tested to further isolate the differences between the right and left valves. First, we conducted a paired t-test to compare the strength of

the right and left valves. Then, we used the paired data to examine the importance of morphological differences between the right and left valves in determining strength. Because their apertures line up, by definition, right and left valves tend to have similar lengths and heights (see Fig. 1A for definitions), but their widths can vary. We therefore examined the role of width in predicting differences between the right and left valves of the same shell by fitting a linear regression of the difference in strength of the right and left valves as a function of their difference in width. This regression was later used in analyzing our fatigue experiments; the fatigue results rely on normalizing the applied fatiguing force relative to the predicted strength of the valve, which we calculated from the strength of the paired valve and the width of both valves.

Fatigue testing

We examined the results of our fatigue experiments using a modified S–N curve, a traditional way to describe the lifetime of a fatigued structure. Classically, the log-transformed applied stress (S) is visualized in terms of the log-transformed number of cycles (N). Often this fatigue resistance curve shows a negative, linear relationship. We did not measure stress, because identifying stress distributions and therefore relevant cross-sectional areas from a whole valve was beyond the scope of this study. Therefore, we adapted this form, examining the log-transformed force in terms of either the log-transformed number of cycles or the log-transformed loading duration.

We tested whether valves experienced fatigue when loaded cyclically, and which morphological traits affected fatigue resistance. We considered the absolute force applied to the valve, using a multiple regression to examine the log-transformed force required to break a valve as a function of the log-transformed number of cycles, valve mass, domedness, relative thickness and a categorical variable indicating right or left valve. We began by including all variables, then excluded non-significant ones. An initial multiple regression model was also tested that included interaction terms for each morphological variable interacting with the log-transformed number of cycles. If non-significant, these interaction terms were excluded. Additionally, we constructed a separate statistical model that considered the applied force relative to a valve's predicted strength, which was calculated as described in 'Strength testing', above, and took valve morphology into account. We fitted a linear regression of the log-transformed relative force as a function of the log-transformed number of cycles. Because the valve's predicted strength took into account valve morphology and differences between right and left valves, those variables were not included in the model. For both the absolute and relative force regression models, shells for which both valves had been strength tested were also included, with the second valve tested being considered the 'fatigued' valve exposed to a single cycle.

We assessed static fatigue resistance and directly compared it with cyclic fatigue resistance. We transformed the number of cycles into a measure of time by multiplying the number of complete cycles by the duration of each cycle and dividing by two, to integrate under the triangular loading/unloading curve. We added to this the duration of the last cycle during which the shell broke, divided by two. Note that for a given valve, all cycles had the same loading/unloading cycle duration, and that the lag time between cycles, when the valve was not loaded, was not included in these calculations. Because of the compliance of the force sensor, depending on the cycle duration, this linear approximation slightly underestimated the duration of the curve. We corrected for this by multiplying the calculated total duration by a correction ratio of: $0.971\times(\text{cycle duration})^{-0.397}$. Valves that broke during the first cycle were excluded from this analysis. We fitted a multiple regression of log-transformed force as a function of log-transformed duration, valve mass, domedness, relative thickness, a categorical variable indicating right or left valve, a categorical variable indicating cyclic or static loading, and the interaction between the log-transformed duration and the categorical variable indicating cyclic or static loading. We began by including all variables, then excluded non-significant ones. An initial multiple regression model was also tested that included interaction terms for each morphological variable interacting with the log-transformed duration. If non-significant, these interaction terms were excluded. As with the cyclic fatigue data, we also constructed a statistical model with the applied force relative to predicted strength, and fitted a multiple regression of the log-transformed relative force as a function of the log-transformed duration, a categorical variable indicating cyclic or static loading, and an interaction term. Non-significant terms were excluded.

Finally, the advantage of dividing by predicted strength is that it takes into account known mechanical properties of a valve's counterpart. We assessed how normalizing the applied force by the predicted strength affected our analyses, by testing whether unexpectedly weak or strong valves were associated with fatigue duration. Specifically, for each strength-tested valve, we calculated how much weaker or stronger it was than expected based on morphology. We calculated the expected strength from the model described in 'Strength testing', above (Fig. 2) and subtracted it from the measured strength. In other words, we calculated the residuals of the strength model. We then tested for a relationship between these residuals of the strength-tested valves and the fatigue duration of the fatigue-tested valves; we fitted a multiple regression of the strength residuals in terms of the log-transformed fatigue duration, a categorical variable indicating cyclic or static loading, and an interaction term.

Self-imposed forces

Minimum closing force

We identified the relationship between the opening force of the hinge and mussel size using two generalized mixed models (fitted in R, nlme, version 3.1.137; https://CRAN.R-project.org/package=nlme). We examined torque on the hinge as a function of shell length with a random effect of individual, and we examined the force of the adductor muscle required to counteract the torque as a function of shell length with a random effect of individual.

Maximum closing force

We fitted a linear regression of the maximum closing force each mussel could generate as a function of shell length. To facilitate comparisons with other kinds of muscle, we divided the force from the muscle by the surface area of the posterior adductor muscle scar to produce a stress value and generated summary statistics.

All statistical analyses were conducted in R (version 3.3.2; http://www.R-project.org/) using RStudio (version 1.1.463; http://www.rstudio.com/). All plots were generated with the R package ggplot2 (version 3.2.1; https://CRAN.R-project.org/package=ggplot2; Wickham, 2009).

RESULTS

Morphological scaling

Scaling relationships of all linear morphological variables with respect to length differed significantly from isometric scaling (Table 1), with longer valves being slightly less tall but relatively wider and thicker.

Journal of Experimental Biology (2020) 223, jeb220277. doi:10.1242/jeb.220277

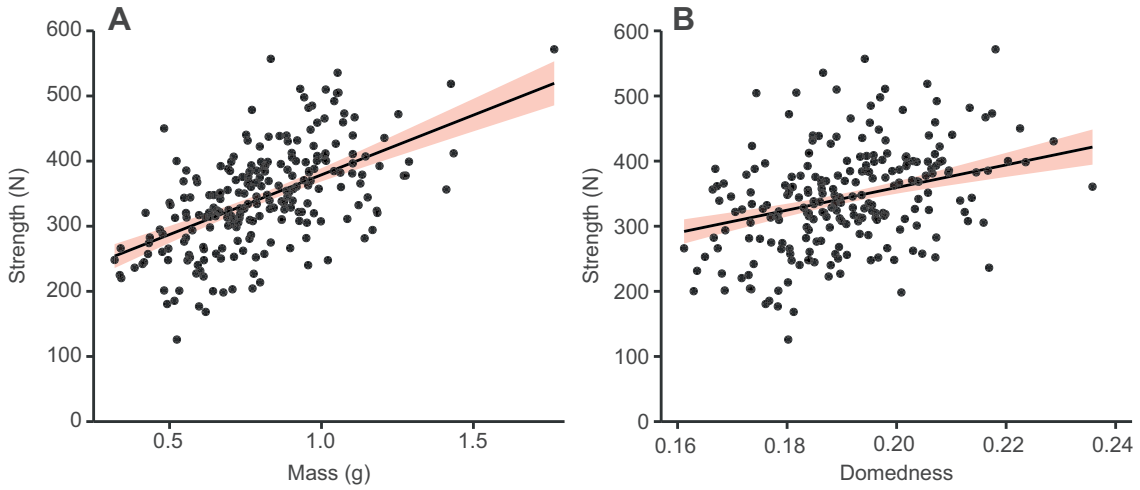

Fig. 2. Mussel valve strength and morphology. Valves that were (A) more massive or (B) more domed (i.e. relatively wide for their length) tended to be stronger. The same valves are represented in both plots; *N*=228 valves. The full statistical model is reported in Table 2. Multiple regression and 95% confidence intervals are plotted with domedness held constant at the average value in A and with mass held constant at the average value in B.

Strength testing

On average, individual undamaged valves broke at 343±78 N (mean±s.d., range 126–572 N, *N*=228 valves). Valve strength tended to increase with valve mass and domedness (ratio of width to length), such that valves that were larger or more domed tended to be stronger (Fig. 2, Table 2). According to the multiple regression, the categorical variable indicating right or left valve was not a significant predictor of strength (Table 2). Right and left valves did not differ in mass (Welch two sample *t*-test: t=0.84, d.f.=225.05, P=0.40), but left valves were slightly more domed than right valves (Welch two sample *t*-test: t=2.46, d.f.=225.75, P<0.05).

In intraindividual paired comparisons, right valves tended to be stronger than left valves (difference in strength: mean±s.d. 33±83 N, *N*=63 pairs of valves; paired *t*-test: t=3.20, d.f.=62, P<0.01). Furthermore, the wider valve in a pair – and, by extension, the more domed – also tended to be stronger [Fig. 3; $F_{1,61}$=12.21, P<0.001; model: ($Strength_R - Strength_L$)=42.6+114.7×($Width_R - Width_L$), where $Strength_R$ and $Strength_L$ are the strength of the right and left valves, respectively, and $Width_R$ and $Width_L$ are the width of the right and left valves, respectively].

Fatigue resistance

Mussel valves experienced fatigue when loaded cyclically (Fig. 4A,B), such that as the number of cycles increased, a lower force was required to break a valve, according to a linear log–log fit (Table 2). Larger, more domed or right valves all tended to be more fatigue resistant (Table 2). No interaction terms of morphological variables with the log-transformed number of cycles were significant (P>0.05), so these terms were excluded from the regression model.

Mussel valves also experienced fatigue when loaded statically, such that lower forces were sufficient to break a valve after a longer period of time (Fig. 4C,D, Table 2). Larger, more domed or right valves were again more fatigue resistant (Table 2). When considering applied force relative to predicted strength, cyclic and static loading caused fatigue on similar time scales (Fig. 4D, Table 2). However, when considering absolute applied force, a model that incorporated less information about the shells, the curves for cyclic and static loading differed slightly but significantly, with static loading having a shallower slope and lower intercept (Fig. 4C, Table 2). No interactions between the other predictor variables and the log-transformed duration were significant in predicting the log-transformed force (P>0.05), so these terms were excluded.

The strength-tested valve counterparts to cyclically loaded valves were neither weaker nor stronger than expected based on size in relation to the loading duration of the fatigued valve (Fig. 5; P=0.26); in contrast, the counterparts to statically loaded valves tended to be increasingly stronger than expected at longer loading durations [Fig. 5; P<0.05; full model: $F_{3,141}$=2.7, P<0.05, R^2=0.05; model for cyclic loading: (strength residual)=12.4–6.4×$\log_{10}$(fatigue duration); model for static loading: (strength residual)=−54.2+9.7×$\log_{10}$(fatigue duration)].

Self-imposed forces

Hinges imposed, on average, a constant opening torque of 46±19 N mm (mean±s.d., *N*=10 mussels for 30 total experiments), which corresponds to the adductor muscle exerting a constant average force of 4.1 N. The hinges of larger mussels opened more forcefully [model: hinge torque (N mm)=−74.1+3.8×shell length (mm), length coefficient: t=4.7, P<0.01], requiring the posterior adductor muscle to generate a larger force, with a marginal effect of size [Fig. 6; model: muscle force (N)=−1.72+0.20×shell length (mm), length coefficient: t=2.2, P=0.057].

Mussel adductor muscles were able to generate a maximum closing force of 31.4 N (maximum force: mean±s.d. 22.6±5.4, *N*=13 mussels for 40 experiments). Larger animals generated a greater maximum force [Fig. 6; model: maximum force (N)=−13.1+1.1×shell length (mm); $F_{1,11}$=15.5, P<0.01, R^2=0.58]. Taking muscle surface area into account, this means the posterior

Table 1. Hypothesis testing of linear scaling of mussel valve morphological variables using confidence intervals from reduced major axis regression

x-variable	*y*-variable	Scaling exponent (*b*)	95% CI
Length	Height	**0.935**	0.882–0.991
Length	Width	**1.134**	1.057–1.218
Length	Thickness	**1.416**	1.271–1.578

All linear morphological variables scaled non-linearly with length. Scaling was tested using the log-transformed allometric scaling equation: $y=ax^b$. Bold values for the scaling exponent (*b*) indicate that 95% confidence intervals (CI) for *b* did not include the null hypothesis of *b*=1, indicating non-linear scaling with P<0.05; *N*=228 valves.

Journal of Experimental Biology (2020) 223, jeb220277. doi:10.1242/jeb.220277

Table 2. Multiple regression models illustrating how mussel shell morphology affected valve strength and valve fatigue resistance

							Coefficients							
Dataset	*F*	d.f.	*N*	*P*	R^2	*y*	Intercept	$\log_{10}$(No. of cycles)	$\log_{10}$(Time)	Mass (g)	Domed-ness	Relative thickness	Valve (right)	Test (static)	Test×$\log_{10}$ (time)
Strength	85.9	2,225	228	<0.001	0.43	Strength	−136	–	–	183§	1737§	*P*=0.22	*P*=0.09	–	–
Cyclic fatigue	130.7	4,151	156	<0.001	0.78	$\log_{10}$(force)	1.945	−0.101§	–	0.278§	1.816§	*P*=0.33	0.031*	–	–
	324.6	1,154	156	<0.001	0.68	$\log_{10}$(force ratio)	−0.008	−0.096§	–	–	–	–	–	–	–
Cyclic & static fatigue	135.6	6,138	145	<0.001	0.86	$\log_{10}$(force)	1.857	–	−0.096§	0.232§	2.098§	*P*=0.75	0.044§	−0.113§	0.029‡
	411.8	1,143	145	<0.001	0.74	$\log_{10}$(force ratio)	−0.083	–	−0.083§	–	–	–	–	*P*=0.56	*P*=0.41

Multiple regression models defined valve fatigue resistance curves and explored the relationship between morphology and a valve's mechanical properties, including strength, cyclic fatigue resistance and static fatigue resistance. For fatigue treatments, we separately created models for the absolute applied force (in N) as well as the applied force relative to the predicted strength (force ratio). Initial models included all appropriate morphological variables. Dashes indicate a variable was not included in the initial model, because it was not applicable or was already accounted for. The *P*-value of a coefficient is reported for variables that were not significant (*P*>0.05). These variables were then excluded from the model, and the reduced model is reported. *P<0.05, ‡P<0.01, §P<0.001.

Fig. 3. Comparison of strength and morphology of right and left valves. When both valves of a shell were individually strength tested, the wider valve tended to be stronger than the narrower one, and the right valve (R) tended to be stronger than the left (L) [$F_{1,61}$=12.21, P<0.001; model: ($Strength_R$–$Strength_L$)= 42.6+114.7×($Width_R$–$Width_L$)]. This relationship was used to predict the strength of one valve from the measured strength of the other, which was necessary for analysis of the fatigue-tested valves (described further in Materials and Methods, 'Statistical analyses'). Line shows linear regression with 95% confidence intervals; N=63 pairs of valves.

adductor muscle generated an average maximum stress of 1.9(±0.4)×10^6 Pa (mean±s.d., range 1.2×10^6–2.4×10^6; equivalent to 190 N cm^{-2}).

DISCUSSION

Valves of the California mussel shell fatigue and fracture under cyclic and static loading such that subcritical forces can break them if applied repeatedly or over long durations (Fig. 4). Although the valves in this study had an average one-time strength of 343±78 N (mean±s.d., maximum 572 N), when fatigued, they broke under much lower forces (lowest tested fatiguing force: 74 N) and across a broad range of time scales: 0.5 s to over 409 days. Fatigue-induced weakening was dramatic at relatively high forces: 80% of the one-time breaking force was sufficient to break valves within 9 cycles or 1.5 s. However, because of the log–log nature of the relationship between force and time to fracture, decreases in required force tapered off in conjunction with dramatic increases in time to fracture; 50% of the one time-breaking force required 1100 cycles or 7 min, and 20% required almost 15 million cycles and over 44 weeks.

Ecological significance

A mussel's fatigue resistance curve allows us to categorize the threat posed by different predatory and environmental forces. To make these comparisons, we make the assumption that our measures of valve mechanical properties roughly represent those of the shell as a whole. Some predators and environmental threats will never rely on fatigue. An otter (Christiansen and Wroe, 2007; Fig. 7) or a storm-hurled boulder (Shanks and Wright, 1986) could fracture shells with a single impact. By contrast, low-magnitude forces would never cause fatigue on ecologically relevant time scales. The force a mussel imposes on itself by pulling its valves shut ranges from 4.6 to 32 N (Fig. 6), which, standardized by muscle cross-sectional area, is typical of other invertebrate muscles (Jewell, 1959; Taylor, 2000). Extrapolating the fatigue resistance curve, the maximum closing force, which is equivalent to 9.1% of the average strength of shells from this experiment, would have to be applied continuously

Journal of Experimental Biology (2020) 223, jeb220277. doi:10.1242/jeb.220277

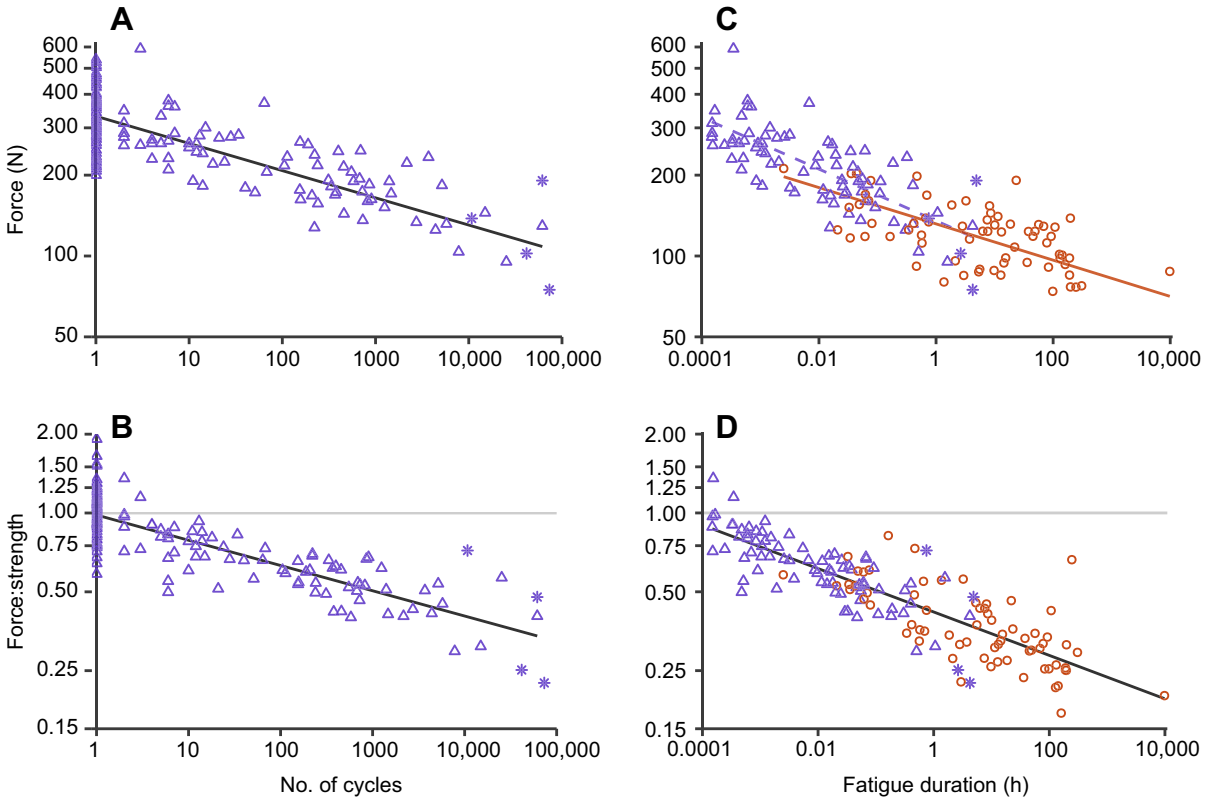

Fig. 4. Valves of mussel shells fatigue under cyclic and static loading. (A,B) The force required to break a valve decreased as a valve was loaded repeatedly. This was true for absolute force (A) and force relative to predicted strength (B). Multiple regressions are shown at average values for all morphological variables (Table 2). The light gray line in B represents a loading force equal to the predicted one-time strength. Purple asterisks indicate that a valve never broke and therefore represent a lower bound of the true number of cycles until breakage. These points were not included in the regression. *N*=156 complete, *N*=4 incomplete tests of individual valves. (C,D) Valves that were loaded cyclically (purple triangles) and statically (red circles) both experienced fatigue, whether considering absolute force (C) or force divided by predicted strength (D). Multiple regressions are shown at average values for all morphological variables (Table 2). Regressions for cyclic (purple dashed line) and static (red solid line) loading differed significantly when considering absolute force (C), but they did not differ when accounting for predicted strength (D) (Table 2). The light gray line in D represents a loading force equal to the predicted strength. Purple asterisks indicate that a valve never broke under cyclic loading and therefore represent a lower bound of the true time until breakage. These points were not included in the regression. Cyclic fatigue: *N*=77 complete, *N*=4 incomplete tests of individual valves; static fatigue: *N*=68 complete tests of individual valves.

for 10,700 years before it would break a typical shell (Fig. 7). Similarly, mussels are constantly being hit by waves. We can estimate the force from drag (F_{drag}) imposed by a moderately sized wave as:

$$F_{drag} = \frac{1}{2}\rho v^2 A C_{drag}, \quad (4)$$

where ρ is the density of seawater (~1025 kg m^{-3}), v is the velocity (10 m s^{-1} for a moderate wave), A is the projected surface area of the broadside of a mussel (measured from photographs to be ~0.00065 m^2 for the larger shells in this experiment) and C_{drag} is the coefficient of drag for a mussel broadside to flow (0.8; Denny et al., 1985). We found a moderately sized wave imposes a drag force of only 27 N, or 7.9% of the average strength, which would have to be applied continuously for 65,900 years to break a shell (Fig. 7). These time scales indicate that not only will these low-magnitude forces never break a mussel shell but also they will not appreciably weaken a shell within the animal's lifetime. In short, the California mussel possesses a robust shell, equipped for many of the chronic stresses of the exposed coast.

However, between high stresses, for which fatigue is unnecessary, and low stresses, for which it is irrelevant, intermediate forces exist that can cause significant fatigue damage. Fatigue can provide a route for predators to kill otherwise inaccessible prey. A large crab (Taylor, 2000) can generate forces sufficient to break a shell in under 4 min (Fig. 7), which, given that crabs are known to pulse when crushing hard-shelled prey (Boulding and LaBarbera, 1986), would be feasible, especially in conjunction with other behavioral strategies they are known to use, like targeting smaller prey or weak points in shell armor (Boulding, 1984; Zipser and Vermeij, 1978). However, the log–log nature of the relationship between required force and force duration highlights the limits of this approach for predators. Possessing a less powerful weapon, like the jaws of the horn shark (an unlikely predator), which can generate half the force of a crab (Huber et al., 2005), increases the required duration to break a shell from minutes to over 6 days.

In addition to predators that, in a single encounter with multiple attacks, can use fatigue to break a shell, mussels face moderate, episodic forces that, across long time scales, could potentially cause accumulating fatigue damage, thus weakening a shell and shortening an animal's life. Failed predation attempts and environmental threats such as impacts from waves and wave-hurled debris during a large storm could fall into this category of causing long-term damage. The threat of these kinds of forces depends on a mussel's ability to sense and repair accumulating fatigue damage. Bivalves can repair large, imminently lethal damage (Meenakshi et al., 1973), and they sense and respond to non-lethal environmental stimuli by modifying shell shape (Leonard et al., 1999; Reimer and Tedengren, 1996). However,

Journal of Experimental Biology (2020) 223, jeb220277. doi:10.1242/jeb.220277

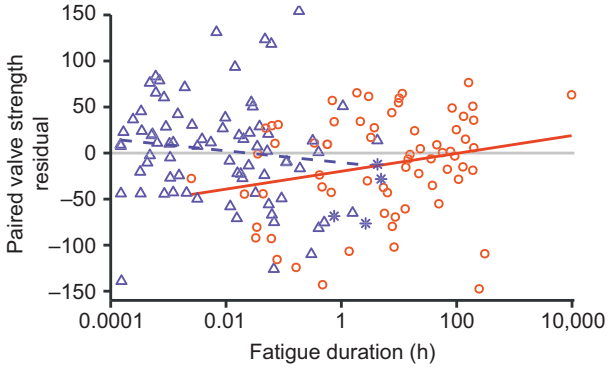

Fig. 5. Strength of counterparts of cyclically and statically loaded valves. Taking advantage of a shell's two-valve morphology, the partner valve of each fatigue-tested valve was strength tested to provide general information about the shell. In the static fatigue treatment (red circles, solid line), valves that broke after shorter durations also tended to have counterparts that were uncharacteristically weak for their size (P<0.05); for cyclically fatigued shells (purple triangles, dashed line), no such relationship existed [P=0.26; full model: $F_{3,141}$=2.7, P<0.05, R^2=0.05; model for cyclic loading: (strength residual)=12.4−6.4×$\log_{10}$(fatigue duration); model for static loading: (strength residual)=−54.2+9.7×$\log_{10}$(fatigue duration)]. Deviation from expected strength based on morphology was quantified as the valve's residual (actual−predicted strength) calculated from the strength model in Table 2. The light gray line represents a residual of 0, with negative y-values indicating uncharacteristically weak valves, and positive y-values indicating uncharacteristically strong valves. Purple asterisks indicate that the fatigue-tested valve never broke and therefore represent a lower bound of the true duration until breakage. These points were not included in the regression. Cyclic fatigue: N=77 complete, N=4 incomplete tests of individual valves; static fatigue: N=68 complete tests of individual valves.

mussels' sensitivity to the micro-damage associated with fatigue is unknown. Other mollusks have been shown to repair fatigue damage (LaBarbera and Merz, 1992; O'Neill et al., 2018), and to patch internally in response to external wear (limpets: Cadée, 1999; O'Neill et al., 2018; pteropods: Peck et al., 2018). The ecological threat of fatiguing forces will depend on the mussel's ability to sense and repair fatigue, as well as the time required to repair the shell, the cost of repair, and the mechanical properties of the shell once repaired.

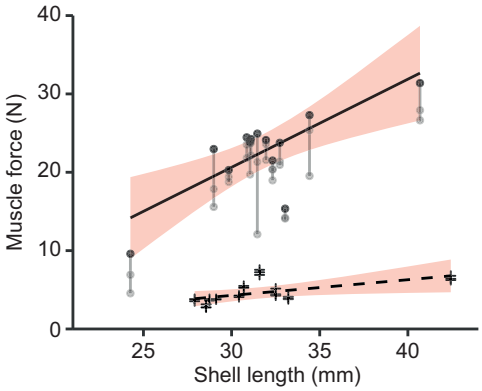

Fig. 6. Mussel shells constantly experience low-magnitude, self-imposed forces that are correlated with shell size. A constant minimum force is imposed by the hinge (black crosses). Dashed line (with 95% confidence intervals) shows a mixed effects model that included individual mussel as a random effect [muscle force (N)=−1.72+0.20×shell length (mm), length coefficient: t=2.2, P=0.057]. N=30 observations from 10 mussels. In response to a force prying the shell open, the adductor muscles generated the maximum possible closing force (circles) to clamp shut. A linear regression (solid line with 95% confidence intervals) was fitted only to the maximum force for each individual (black circles), though other measures for each individual (gray circles) are shown [maximum force (N)=−13.1+1.1×shell length (mm); $F_{1,11}$=15.5, P<0.01, R^2=0.58]. Gray lines connect repeat measures. N=40 observations from 13 mussels.

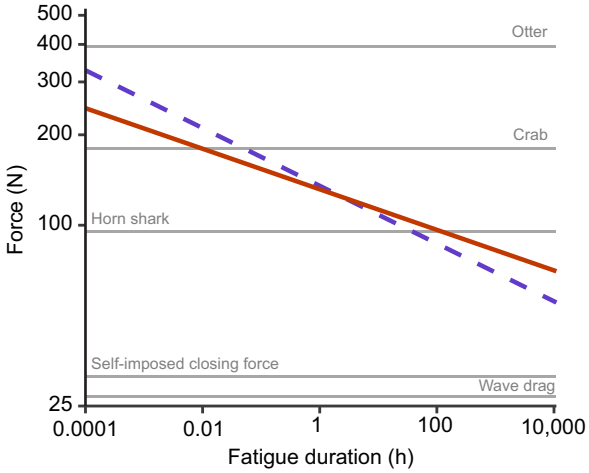

Fig. 7. The ecological relevance of fatigue depends on the magnitude of the applied force for cyclic and static fatigue. The regressions for cyclic fatigue (dashed purple line) and static fatigue (solid red line) correspond to Fig. 4C and Table 2. Note, the static loading regression does not account for patterns in the shell strength (Fig. 5) that could result in an artificially shallow slope. From top to bottom, forces represent: otter bite (Christiansen and Wroe, 2007), crab crushing claw (Taylor, 2000), horn shark bite (Huber et al., 2005), the maximum self-imposed closing force (Fig. 6) and drag from a moderate wave (see 'Discussion' for calculation).

Shell and weapon morphology

Certain morphological features consistently improved a shell's fracture resistance. Valves that were larger (more massive) and more domed tended both to be stronger and to withstand a longer duration at a given force (Table 2). It is important to note that these morphological features changed the intercept but not the slope of the fatigue-resistance curves; larger and more domed valves were generally stronger, but maintained the same underlying relationship with fatigue (Table 2). Valves that were relatively thick for their size were neither stronger nor more fatigue resistant (Table 2). We hesitate, though, to make broad conclusions about the importance of thickness to strength or fatigue resistance, because we tested only minimally damaged shells, with, therefore, minimal variation in thickness due to wear, restructuring or repair. How wear and remodeling affect shell mechanical properties remains an exciting avenue for future research.

Intriguingly, right valves showed a slight but significant superiority over left valves in almost all strength and fatigue-resistance tests (Fig. 3, Table 2). We were unable to identify a morphological cause of this mechanical difference. However, we measured only a standard suite of gross morphological variables. It is possible that the valves differed in features, such as curvature or microstructure, that we did not measure. Only in the unpaired strength data were right and left valves not statistically significantly different, though they did approach marginal significance (Table 2). This lack of difference could indicate a few things. First, the difference in strength between right and left valves in the paired data is small (mean difference of 33 N) and therefore potentially invisible in the statistically less powerful unpaired data. Second, left valves in the unpaired data were significantly more domed than right valves. Given that domedness correlated with strength, it is

possible that differences in domedness obscure population-wide differences in strength. It is, in fact, surprising that left valves, which were more domed, were not stronger than right, suggesting some still unidentified asymmetric feature.

Although our findings suggest how shell morphology affects fatigue resistance, we did not consider the role of weapon morphology. We chose to use a simple and consistent crushing surface for all of our mechanical testing, because we wanted to directly compare fatigue across a broad range of forces and time scales. Furthermore, the flat surface used resembles the classic and broadly used apparatus for testing shell strength (described in Vermeij and Currey, 1980). However, in interpreting our findings ecologically, it is necessary to consider the crushing surface, which can affect the results of mechanical testing (Crofts and Summers, 2014). Integrating research on fatigue resistance across a variety of crushing surfaces would offer potential new insight into the ecological significance of fatigue.

Cyclic versus static loading

The fatigue resistance curves for cyclic and static loading did not differ when considering applied force relative to strength (Fig. 4D, Table 2), suggesting that cycling is not necessary for fatigue in shells; all that matters is the duration for which a load is applied. This was not the case for the fatigue-resistance curve of absolute applied force (Fig. 4C, Table 2), for which the slopes of cyclic and static curves differed slightly but significantly. However, this model failed to take into account that at intermediate loading durations the statically loaded shells, in particular, happened to be weaker than expected based on size. This pattern could drive the differences that we saw in the slopes of the cyclic and static fatigue curves, making the static fatigue curve shallower than is true for mussel valves in general. When the strength of partner valves was taken into account by dividing by predicted shell strength, the cyclic and static loading curves were statistically indistinguishable (Table 2).

That loading duration matters more for determining the course of fatigue in shells than the number of cycles is surprising, when considering other biological materials. Fatigue of human and bovine cortical bone in tension at subcritical stresses has similarly been shown to be primarily time, as opposed to cycle, dependent, indicating creep rupture as the underlying mechanism (Caler and Carter, 1989; Carter and Caler, 1983; Zioupos et al., 2001). However, this finding is by no means broadly true across biological systems or loading regimes. The lifetime of human cortical or bovine trabecular bone fatigued in compression is largely cycle dependent and not attributable to creep (Caler and Carter, 1989; Moore et al., 2004). Fracture of wallaby tail tendons is neither purely cycle dependent nor purely time dependent (Wang and Ker, 1995; Wang et al., 1995). Given the varied relationship between fracture under cyclic and static loading across systems, we were surprised by our finding that fatigue fracture in intact mussel valves is time dependent. Mussel shells have a complex, multilayered structure, and the distribution of forces across all the layers of an intact domed shell in compression is notably more complex than the distribution of forces in a machined strip tested in tension or compression. Different portions of a compressed shell will experience tension, compression or shear. Further work is required to identify what portions of the shell are most strongly affected by fatigue and to pinpoint where fracture is initiated and how it progresses. Additional fatigue testing, either at varied loading rates or by maintaining the maximum load, could more thoroughly isolate the relative importance of cycle count versus loading duration. How these variables affect crack propagation through the shell as well as the mussel's ability to respond remain unanswered.

The finding that duration determines the fatigue lifetime of valves of mussel shells has both experimental and ecological implications. Experimentally, it validates the use of a variety of different crushing apparatuses to facilitate testing across a broad range of temporal scales and force magnitudes, which can be valuable in working around the limitations of specific testing devices. Incorporating the results of our cyclic and static loading devices offered insight on a broader range of force magnitudes and time scales than were testable with either device alone. The importance of loading duration also presents a new perspective to highlight the importance when testing shells of carefully selecting loading rates, which are known to alter mechanical results (Burnett and Belk, 2018). Slower loading rates will allow more time at any given force for damage to accumulate, although this can be taken into account with a well-defined fatigue-resistance curve. Ecologically, the importance of loading duration suggests that all different kinds of forces that mussels might encounter, from cyclic to chronic stresses, can be considered together to understand how damage accumulates in shells, and by extension to shed light on the lifetime of a single mussel.

Broader context and conclusions

We have shown in a bivalve model that a broad range of force magnitudes can weaken and ultimately break a shell, and we demonstrated the ecological utility of considering how a shell fatigues. Quantifying shells' fatigue resistance allowed us to compare the resistance of shell armor to a full spectrum of potential threats. We considered not just the highest magnitude forces a mussel might encounter but instead incorporated different kinds of fatiguing forces that act throughout a mussel's life, which suggested two key ecological contexts for fatigue. On short time scales, fatigue may allow some predators to fracture otherwise inaccessible prey, and on long time scales, moderate episodic forces may fatigue shells, which could prove lethal, depending on the mussel's capacity for repair.

When interpreting the ecological significance of mussels' fatigue resistance, the potential repercussions of climate change loom large. *Mytilus* mussels, like other animals with calcium carbonate shells, are particularly hard hit by acidifying and warming oceans, as demonstrated by changes in shell morphology (Fitzer et al., 2015a; Gaylord et al., 2011), microstructure (Fitzer et al., 2014; Hahn et al., 2012; Li et al., 2015) and chemical composition (Li et al., 2015). *Mytilus* shells also show changes in mechanical properties, including strength (Gaylord et al., 2011; Li et al., 2015; Mackenzie et al., 2014), maximum deformation before failure (Mackenzie et al., 2014), and stiffness and hardness (Fitzer et al., 2015b). It is further possible that changing ocean conditions could shift fatigue-resistance curves, altering the intercept or slope, and increasing the mussel's susceptibility to fatigue. Meanwhile, decreased calcification rates (Fitzer et al., 2014; Li et al., 2015) and an increased cost of calcification (Melzner et al., 2011) associated with acidified oceans could limit a mussel's ability to repair a fatigued shell. A decrease in fatigue resistance could further coincide with increased fatiguing threats from waves and storms with changing weather patterns. Further testing is required to understand how mussels will cope with low-magnitude mechanical stresses in a changing ocean.

In this study, we considered only the California mussel. However, this method of analysis may provide a compelling perspective in other systems. The range of forces the California mussel encounters in the wave-swept rocky intertidal zone of exposed coasts differs from those encountered by a mollusk in calm but predator-filled waters, or an infaunal bivalve, protected from many kinds of predation but compacted by sediment and relying on its shell to

burrow. Quantifying and contextualizing fatigue resistance across more species could offer new insight into evolutionary patterns of shell form. Because shells can be weakened by subcritical forces, we highlight the potentially powerful selective force that subcritical stresses can play in shaping shell form.

Acknowledgements
We are grateful to John Lee and Tom Rolander for invaluable assistance with building and designing experimental testing devices, and Tom Hata for help with MATLAB code. Pablo Absalon assisted with pilot experiments, and Benjamin Burford, Nicole Moyen, Elora López and Giovanni Fusco helped with data collection. We thank Jeremy Goldbogen, Chris Lowe and Jonathan Payne for feedback on the research, and Benjamin Burford, Nicole Moyen and two anonymous reviewers for feedback on the manuscript.

Competing interests
The authors declare no competing or financial interests.

Author contributions
Conceptualization: R.L.C., M.W.D.; Methodology: R.L.C., M.W.D.; Software: R.L.C.; Validation: R.L.C.; Formal analysis: R.L.C.; Investigation: R.L.C.; Resources: M.W.D.; Data curation: R.L.C.; Writing - original draft: R.L.C.; Writing - review & editing: R.L.C., M.W.D.; Visualization: R.L.C.; Funding acquisition: R.L.C., M.W.D.

Funding
This research was funded by a National Science Foundation grant (IOS-1655529) to M.W.D. and a grant from the Dr Earl H. Myers and Ethel M. Myers Oceanographic and Marine Biology Trust to R.L.C.

Data availability
Data are available from Mendeley Data: doi:10.17632/ddk4mhhfwc.1

References
Blundon, J. A. and Vermeij, G. J. (1983). Effect of shell repair on shell strength in the gastropod *Littorina irrorata*. *Mar. Biol.* **76**, 41-45. doi:10.1007/BF00393053
Boulding, E. G. (1984). Crab-resistant features of shells of burrowing bivalves: decreasing vulnerability by increasing handling time. *J. Exp. Mar. Biol. Ecol.* **76**, 201-223. doi:10.1016/0022-0981(84)90189-8
Boulding, E. G. and LaBarbera, M. (1986). Fatigue damage: repeated loading enables crabs to open larger bivalves. *Biol. Bull.* **171**, 538-547. doi:10.2307/1541622
Bourdeau, P. E. (2010). An inducible morphological defence is a passive by-product of behaviour in a marine snail. *Proc. R. Soc. B* **277**, 455-462. doi:10.1098/rspb.2009.1295
Burnett, N. P. and Belk, A. (2018). Compressive strength of *Mytilus californianus* shell is time-dependent and can influence the potential foraging strategies of predators. *Mar. Biol.* **165**, 42. doi:10.1007/s00227-018-3298-y
Buschbaum, C., Buschbaum, G., Schrey, I. and Thieltges, D. W. (2007). Shell-boring polychaetes affect gastropod shell strength and crab predation. *Mar. Ecol. Prog. Ser.* **329**, 123-130. doi:10.3354/meps329123
Cadée, G. C. (1999). Shell damage and shell repair in the Antarctic limpet *Nacella concinna* from King George Island. *J. Sea Res.* **41**, 149-161. doi:10.1016/S1385-1101(98)00042-2
Caler, W. E. and Carter, D. R. (1989). Bone creep-fatigue damage accumulation. *J. Biomech.* **22**, 625-635. doi:10.1016/0021-9290(89)90013-4
Campbell, D. B. (1987). A test of the energy maximization premise of optimal foraging theory. In *Foraging Behavior* (ed. A. C. Kamil, J. R. Krebs and H. R. Pulliam), pp. 143-171. New York, NY: Plenum Press.
Carter, D. R. and Caler, W. E. (1983). Cycle-dependent and time-dependent bone fracture with repeated loading. *J. Biomech. Eng.* **105**, 166-170. doi:10.1115/1.3138401
Christiansen, P. and Wroe, S. (2007). Bite forces and evolutionary adaptations to feeding ecology in carnivores. *Ecology* **88**, 347-358. doi:10.1890/0012-9658(2007)88[347:BFAEAT]2.0.CO;2
Crane, R. L., Cox, S. M., Kisare, S. A. and Patek, S. N. (2018). Smashing mantis shrimp strategically impact shells. *J. Exp. Biol.* **221**, 176099. doi:10.1242/jeb.176099
Crofts, S. B. and Summers, A. P. (2014). How to best smash a snail: the effect of tooth shape on crushing load. *J. R. Soc. Interface* **11**, 20131053. doi:10.1098/rsif.2013.1053
Currey, J. D. (1998). Mechanical properties of vertebrate hard tissues. *Proc. Instn. Mech. Engrs. Part H* **212**, 399-411. doi:10.1243/0954411981534178
Currey, J. D. and Brear, K. (1984). Fatigue fracture of mother-of-pearl and its significance for predatory techniques. *J. Zool. London* **204**, 541-548. doi:10.1111/j.1469-7998.1984.tb02348.x
Dayton, P. K. (1971). Competition, disturbance, and community organization: the provision and subsequent utilization of space in a rocky intertidal community. *Ecol. Monogr.* **41**, 351-389. doi:10.2307/1948498
Denny, M. W., Daniel, T. L. and Koehl, M. A. R. (1985). Mechanical limits to size in wave-swept organisms. *Ecol. Monogr.* **55**, 69-102. doi:10.2307/1942526
Denny, M., Mach, K., Tepler, S. and Martone, P. (2013). Indefatigable: an erect coralline alga is highly resistant to fatigue. *J. Exp. Biol.* **216**, 3772-3780. doi:10.1242/jeb.091264
Fisher, J. A. D. (2010). Parasite-like associations in rocky intertidal assemblages: implications for escalated gastropod defenses. *Mar. Ecol. Prog. Ser.* **399**, 199-209. doi:10.3354/meps08352
Fitzer, S. C., Phoenix, V. R., Cusack, M. and Kamenos, N. A. (2014). Ocean acidification impacts mussel control on biomineralisation. *Sci. Rep.* **4**, 6218. doi:10.1038/srep06218
Fitzer, S. C., Vittert, L., Bowman, A., Kamenos, N. A., Phoenix, V. R. and Cusack, M. (2015a). Ocean acidification and temperature increase impact mussel shell shape and thickness: problematic for protection? *Ecol. Evol.* **5**, 4875-4884. doi:10.1002/ece3.1756
Fitzer, S. C., Zhu, W., Tanner, K. E., Phoenix, V. R., Kamenos, N. A. and Cusack, M. (2015b). Ocean acidification alters the material properties of *Mytilus edulis* shells. *J. R. Soc. Interface* **12**, 20141227. doi:10.1098/rsif.2014.1227
Gaylord, B., Hill, T. M., Sanford, E., Lenz, E. A., Jacobs, L. A., Sato, K. N., Russell, A. D. and Hettinger, A. (2011). Functional impacts of ocean acidification in an ecologically critical foundation species. *J. Exp. Biol.* **214**, 2586-2594. doi:10.1242/jeb.055939
Gosline, J. M. (2018). *Mechanical Design of Structural Materials in Animals*. Princeton, NJ: Princeton University Press.
Hahn, S., Rodolfo-Metalpa, R., Griesshaber, E., Schmahl, W. W., Buhl, D., Hall-Spencer, J. M., Baggini, C., Fehr, K. T. and Immenhauser, A. (2012). Marine bivalve shell geochemistry and ultrastructure from modern low pH environments: environmental effect versus experimental bias. *Biogeosciences* **9**, 1897-1914. doi:10.5194/bg-9-1897-2012
Huber, D. R., Eason, T. G., Hueter, R. E. and Motta, P. J. (2005). Analysis of the bite force and mechanical design of the feeding mechanism of the durophagous horn shark *Heterodontus francisci*. *J. Exp. Biol.* **208**, 3553-3571. doi:10.1242/jeb.01816
Jewell, B. R. (1959). The nature of the phasic and the tonic responses of the anterior byssal retractor muscle of *Mytilus*. *J. Physiol.* **149**, 154-177. doi:10.1113/jphysiol.1959.sp006332
Kolmann, M. A., Crofts, S. B., Dean, M. N., Summers, A. P. and Lovejoy, N. R. (2015). Morphology does not predict performance: jaw curvature and prey crushing in durophagous stingrays. *J. Exp. Biol.* **218**, 3941-3949. doi:10.1242/jeb.127340
LaBarbera, M. and Merz, R. A. (1992). Postmortem changes in strength of gastropod shells: evolutionary implications for hermit crabs, snails, and their mutual predators. *Paleobiology* **18**, 367-377. doi:10.1017/S0094837300010940
Leonard, G. H., Bertness, M. D. and Yund, P. O. (1999). Crab predation, waterborne cues, and inducible defenses in the blue mussel, *Mytilus edulis*. *Ecology* **80**, 1-14. doi:10.1890/0012-9658(1999)080[0001:CPWCAI]2.0.CO;2
Li, S., Liu, C., Huang, J., Liu, Y., Zheng, G., Xie, L. and Zhang, R. (2015). Interactive effects of seawater acidification and elevated temperature on biomineralization and amino acid metabolism in the mussel *Mytilus edulis*. *J. Exp. Biol.* **218**, 3623-3631. doi:10.1242/jeb.126748
Mach, K. J. (2009). Mechanical and biological consequences of repetitive loading: crack initiation and fatigue failure in the red macroalga *Mazzaella*. *J. Exp. Biol.* **212**, 961-976. doi:10.1242/jeb.026989
Mach, K. J., Nelson, D. V. and Denny, M. W. (2007). Techniques for predicting the lifetimes of wave-swept macroalgae: a primer on fracture mechanics and crack growth. *J. Exp. Biol.* **210**, 2213-2230. doi:10.1242/jeb.001560
Mach, K. J., Tepler, S. K., Staaf, A. V., Bohnhoff, J. C. and Denny, M. W. (2011). Failure by fatigue in the field: a model of fatigue breakage for the macroalga *Mazzaella*, with validation. *J. Exp. Biol.* **214**, 1571-1585. doi:10.1242/jeb.051623
Mackenzie, C. L., Ormondroyd, G. A., Curling, S. F., Ball, R. J., Whiteley, N. M. and Malham, S. K. (2014). Ocean warming, more than acidification, reduces shell strength in a commercial shellfish species during food limitation. *PLoS ONE* **9**, e86764. doi:10.1371/journal.pone.0086764
Meenakshi, V. R., Blackwelder, P. L. and Wilbur, K. M. (1973). An ultrastructural study of shell regeneration in *Mytilus edulis* (Mollusca: Bivalvia). *J. Zool. London* **171**, 475-484. doi:10.1111/j.1469-7998.1973.tb02229.x
Melzner, F., Stange, P., Trübenbach, K., Thomsen, J., Casties, I., Panknin, U., Gorb, S. N. and Gutowska, M. A. (2011). Food supply and seawater pCO_2 impact calcification and internal shell dissolution in the blue mussel *Mytilus edulis*. *PLoS ONE* **6**, e24223. doi:10.1371/journal.pone.0024223
Moore, T. L. A., O'Brien, F. J. and Gibson, L. J. (2004). Creep does not contribute to fatigue in bovine trabecular bone. *J. Biomech. Eng.* **126**, 321-329. doi:10.1115/1.1762892
O'Neill, M., Mala, R., Cafiso, D., Bignardi, C. and Taylor, D. (2018). Repair and remodelling in the shells of the limpet *Patella vulgata*. *J. R. Soc. Interface* **15**, 20180299. doi:10.1098/rsif.2018.0299

Paine, R. T. (1966). Food web complexity and species diversity. *Am. Nat.* **100**, 65-75. doi:10.1086/282400
Peck, V. L., Oakes, R. L., Harper, E. M., Manno, C. and Tarling, G. A. (2018). Pteropods counter mechanical damage and dissolution through extensive shell repair. *Nat. Commun.* **9**, 264. doi:10.1038/s41467-017-02692-w
Preston, S. J., Revie, I. C., Orr, J. F. and Roberts, D. (1996). A comparison of the strengths of gastropod shells with forces generated by potential crab predators. *J. Zool. London* **238**, 181-193. doi:10.1111/j.1469-7998.1996.tb05388.x
Pro, J. W. and Barthelat, F. (2019). The fracture mechanics of biological and bioinspired materials. *MRS Bull.* **44**, 46-52. doi:10.1557/mrs.2018.324
Reimer, O. and Tedengren, M. (1996). Phenotypical improvement of morphological defences in the mussel *Mytilus edulis* induced by exposure to the predator *Asterias rubens*. *Oikos* **75**, 383-390. doi:10.2307/3545878
Schneider, C. A., Rasband, W. S. and Eliceiri, K. W. (2012). NIH Image to ImageJ: 25 years of image analysis. *Nat. Methods* **9**, 671-675. doi:10.1038/nmeth.2089
Shanks, A. L. and Wright, W. G. (1986). Adding teeth to wave action: the destructive effects of wave-borne rocks on intertidal organisms. *Oecologia* **69**, 420-428. doi:10.1007/BF00377065
Suchanek, T. H. (1979). The *Mytilus californianus* community: studies on the composition, structure, organization, and dynamics of a mussel bed. *PhD thesis*, University of Washington, Seattle, WA, USA.
Suresh, S. (1998). *Fatigue of Materials*, 2nd edn. Cambridge, UK: Cambridge University Press.
Taylor, G. M. (2000). Maximum force production: why are crabs so strong? *Proc. R. Soc. B* **267**, 1475-1480. doi:10.1098/rspb.2000.1167
Taylor, D. (2016). Impact damage and repair in shells of the limpet *Patella vulgata*. *J. Exp. Biol.* **219**, 3927-3935. doi:10.1242/jeb.149880
Vermeij, G. J. and Currey, J. D. (1980). Geographical variation in the strength of Thaidid snail shells. *Biol. Bull.* **158**, 383-389. doi:10.2307/1540864
Wang, X. T. and Ker, R. F. (1995). Creep rupture of wallaby tail tendons. *J. Exp. Biol.* **198**, 831-845.
Wang, X. T., Ker, R. F. and Alexander, R. M. (1995). Fatigue rupture of wallaby tail tendons. *J. Exp. Biol.* **198**, 847-852.
Wickham, H. (2009). *ggplot2: Elegant Graphics for Data Analysis*. New York, NY: Springer-Verlag.
Zioupos, P., Currey, J. D. and Casinos, A. (2001). Tensile fatigue in bone: are cycles-, or time to failure, or both, important? *J. Theor. Biol.* **210**, 389-399. doi:10.1006/jtbi.2001.2316
Zipser, E. and Vermeij, G. J. (1978). Crushing behavior of tropical and temperate crabs. *J. Exp. Mar. Biol. Ecol.* **31**, 155-172. doi:10.1016/0022-0981(78)90127-2